Printed in the Republic of Korea
ANALYTICAL SCIENCE & TECHNOLOGY
Vol. 36 No. 2, 59-69, 2023
https://doi.org/10.5806/AST.2023.36.2.59

Review

Metal complexes of alizarin and their biological and industrial applications: A literature review

Laith Jumaah Al-Gburi and Taghreed H. Al-Noor★

Department of Chemistry, College of Education for Pure Sciences – Ibn Al-Haitham, University of Baghdad, Iraq

(Received October 26, 2022; Revised November 4, 2022; Accepted December 13, 2022)

1. Introduction

Alizarin is one of the popularly used and wide separated compounds with a chemical name (1,2-dihydroxy-9,10-anthraquinone) which belong to the anthraquinones family that contain three aromatic conjugated rings and in the central rings it contains two ketonic groups.[1] Huge attention and high interests are focused on theoretically and experimentally investigating the alizarin and anthraquinones in general. One of the applications the alizarin possesses like other anthraquinone compounds is dying and pigment usages as a chromophore which still extending significantly.[2] Some of the other usages of alizarin are restoring the artwork,[3] harvesting solar energy,[4] and in analytical chemistry.[5] Alizarin is used to aid the anti-tumor drug[6,7] such as Adriamycin drug as anti-genotoxic compound.[8] Other anthraquinones are common for their medical applications[9-13] as well as their usages as analytical reagent because of the ability of complexation such as dihydroxy-anthraquinones.[14,15]

Alizarin compound as well as its derivatives are commonly used as cations colorimetric reagents. The two OH groups that are located in 1- and 2-positions from the quinoid oxygen gives the alizarin its suitability for forming chelation with metal ions. [16,17] Many researchers investigated the usage of alizarin as a detection agent for determining number of transitional metals[18-21] as well as determining the stability constant for the ligand and its complexes.[22] It is very easy for the dye to form complexes with high stability which gives these complexes its importance in a variety of applications.[23,24] In this review, we present the latest studies that investigate the properties of alizarin and its derivatives as well as their complexes with a wide range of metal ions in terms of preparation, characterization, structural optimization, industrial and medicinal application.

2. Alizarin-Metal Complexes

2.1. Alizarin complex formed with alkali metal hydroxides

Jeliński and Cysewski (2016) investigate the color and structures of alizarin in forms of complexes with alkali metal using computational and quantum calculations methods in methanol solution. Single Gaussian-like band of DFT method was used to predict the color of studies compounds which was very useful for observing the color differences between the experimental and computed values. They found that the alizarin either bind to alkali metal hydroxide through the oxygen atoms of the two OH- groups or one of the hydroxyl groups and the other will be

★ Corresponding author
Phone : +964-1-778-7086, +964-1-778-7080
E-mail : laith.jumaa1105a@ihcoedu.uobaghdad.edu.iq

This is an open access article distributed under the terms of the Creative Commons Attribution Non-Commercial License (http://creativecommons.org/licenses/by-nc/3.0) which permits unrestricted non-commercial use, distribution, and reproduction in any medium, provided the original work is properly cited.

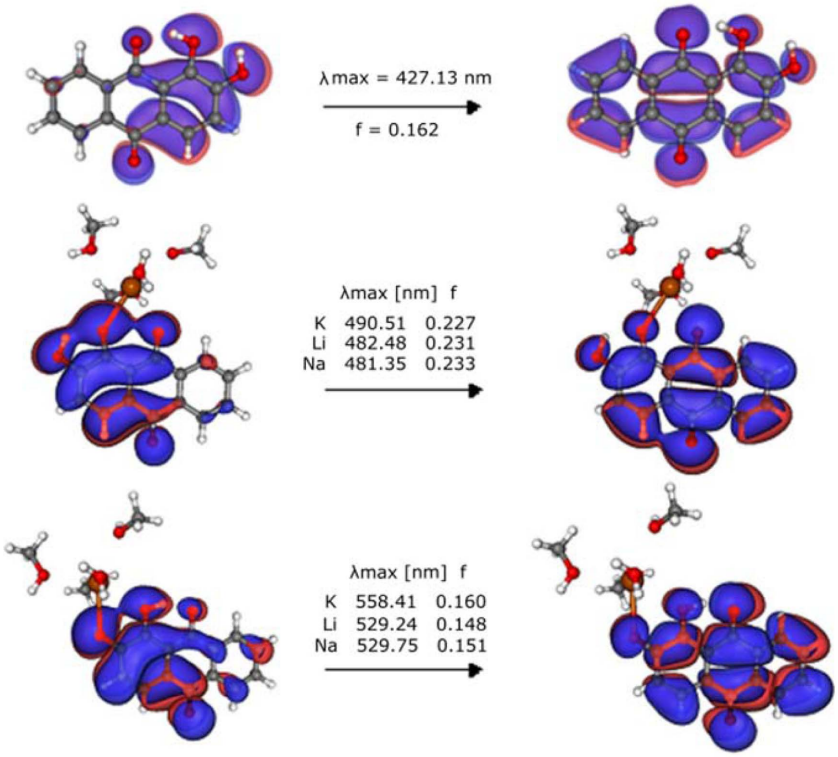

Fig. 1. Electronic spectra and molecular models of alizarin and its complexes with different alkali metal hydroxides.[1]

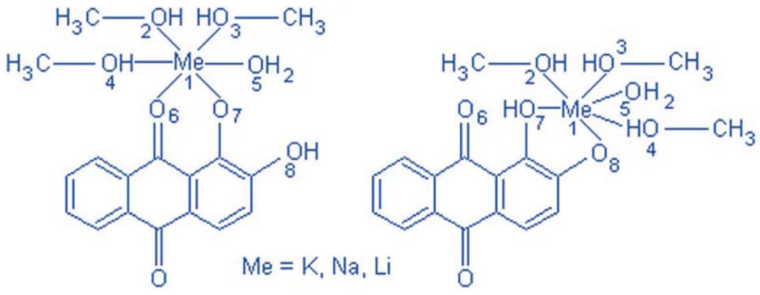

Fig. 2. The proposed structures of the studies complexes with different linkage positions.[1]

connected to three molecules of methanol as illustrated in *Fig.* 1 and *Fig.* 2. As a result, when considering the spectroscopic transitions of the studied complexes, two electronic transitions must be considered. The atomic properties of alkali metal were correlated with calculated bond lengths and angles as well as accurately predicted Pauling electronegativity, atomic radius, molar mass, and other geometric properties of the studied ligand and prepared complexes. The resulted trends of the relationship between the bond lengths and angles, molar mass, and atomic radius are obtained to be possessing positive values, whereas, the electronegativity for the similar trends is having negative values. It can be concluded from this study the efficiency of theoretical calculations for the prediction of the macroscopic properties such as colors.[1]

2.2. Alizarin – lanthanide(Ⅲ) complexs for detecting fluoride

Martínez-Vargas et al. (2011) studied the formation

of alizarin complexes (ALC) with lanthanide ions such as La(III), Y(III), and Eu(III) in a potentiometric titrations in DMSO. The study reveals that binuclear complexes were formed with completely deprotonated (L) and monoprotonated (LH) types of ligands with the following formula M_2L_2H, $M_2L_2H_2$, and M_2L_2. In acidic medium, mononuclear complexes were observed for La(III) complexes with LaLH formula. Adding fluoride for the titration of similar mixtures shifted the complexes' distribution profile with different forms of protonated ALC, with stronger shifting in distribution for deprotonated alizarin with La(III) complexes which explains why blue color species appears in acid mediums which make these complexes applicable for fluoride quantitative determination. The distinctive properties of La(III)–ALC–fluoride complexes can be attributed to several factors such as the conversion of LaLH to La_2L_2HF that induced by fluoride in pH=3, complexes of La(III)– ALC are highly affinitive to fluoride, and mutual influence of ALC ligands and fluoride in ternary lanthanide(III) complexes. This effect can be linked to the changes in coordination number of the metals which enhance the absorbance of La_2L_2HF compared to La_2L_2H. [25]

2.3. Alizarin complexes with copper, cobalt and nickel ions in micellar media

Jumean et al. (2014) tracked the interaction of alizarin violet (AVN) spectrophotometrically with three different transition metals in micellar and water solutions

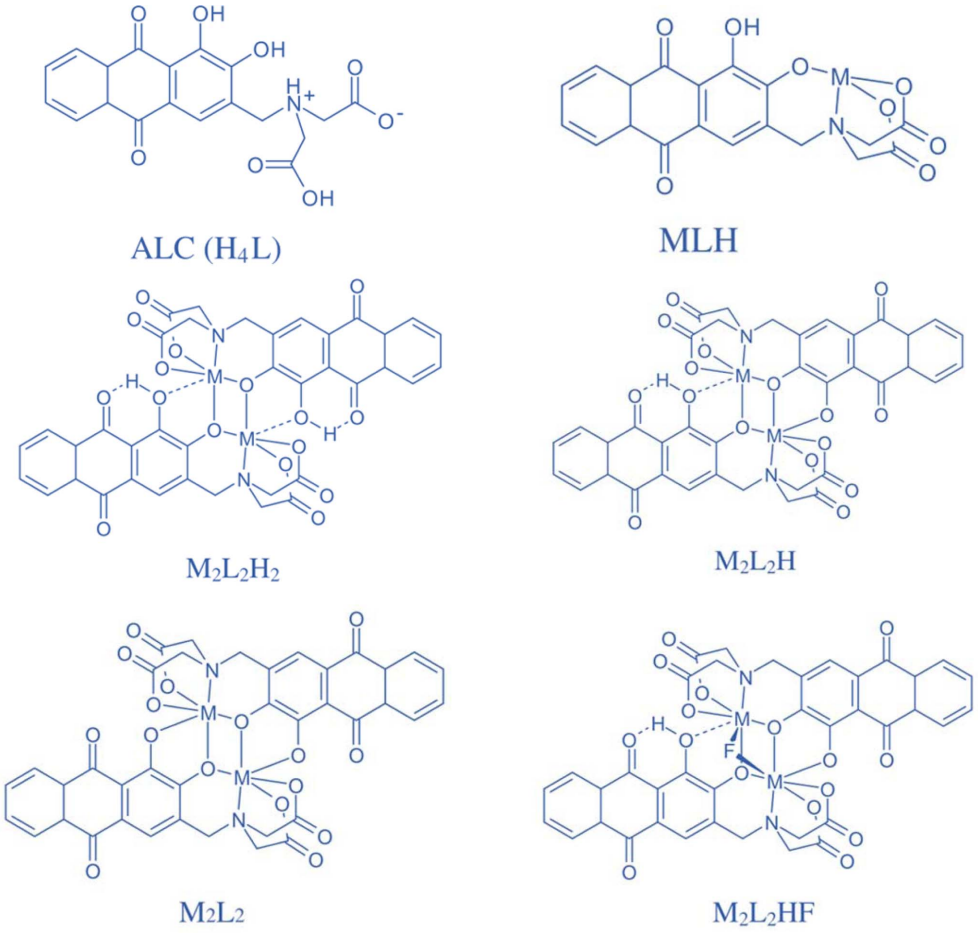

Fig. 3. Chemical structures of tetra protonated forms of ALC and proposed structures of lanthanide complexes with (H_4L), (MLH), ($M_2L_2H_2$), (M_2L_2H), (M_2L_2), and (M_2L_2HF).[25]

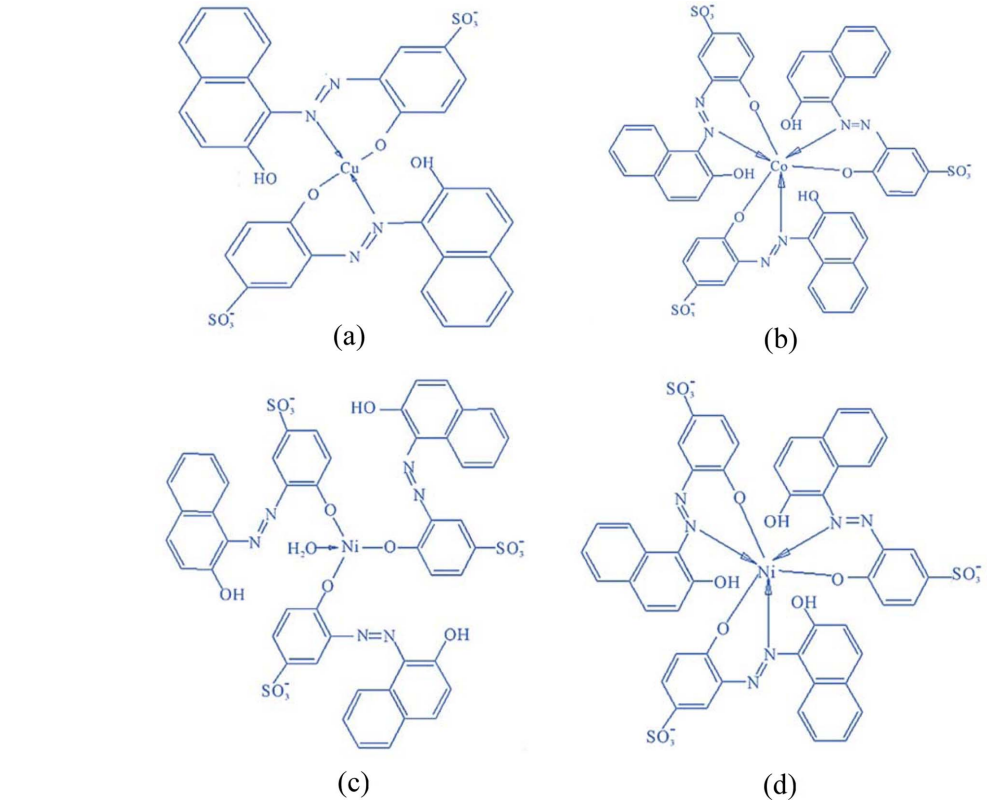

Fig. 4. Chemical structures of (a) Cu^{2+}-AVN complex "square planar", (b) Co^{2+}-AVN complex "octahedral", (c) Ni^{2+}-AVN complex "square planar", and (d) Ni^{2+}-AVN complex "octahedral".[26]

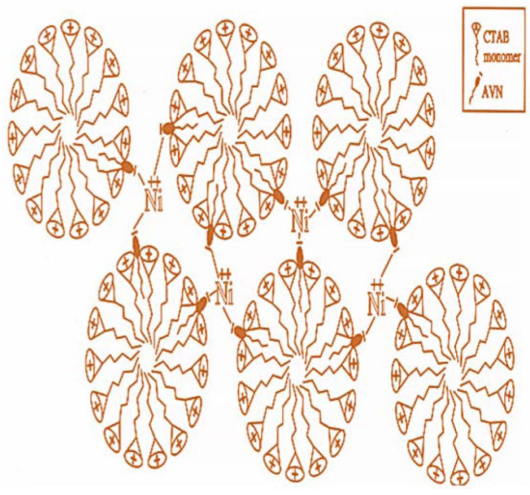

Fig. 5. Ni^{2+}-AVN formation mode in micellar CTAB.[26]

of the nonionic triton X-100 (TX-100), the anionic sodium dodecyl sulfate (SDS), and cationic cetyltrimethylammonium bromide (CTAB). The stoichiometric ratios of metal ion complexes with AVN were obtained using the method of continuous variation and mole ratio. They found that the dye to metal ratios were 1:1, 1:3, and 1:2 for Ni^{2+}, Co^{2+}, and Cu^{2+} complexes in water, respectively. In micellar CTAB, however, they notice the change in the ratio to 1:3 for Ni^{2+} complexes (*Fig.* 5). There are no changes in the other ratios when it comes to all the micellar solutions. The mentioned ratios were explained according to the structural properties. The proposed chemical structures of studied complexes are illustrated in *Fig.* 4.[26]

2.4. Electrochemical behaviors of alizarin chromium (VI) complex

Furtado et al. (2019) investigate, for the first time, the alizarin (Alz) and its metal complex with Cr(VI) which adsorbed on the surface of edge-plane pyrolytic

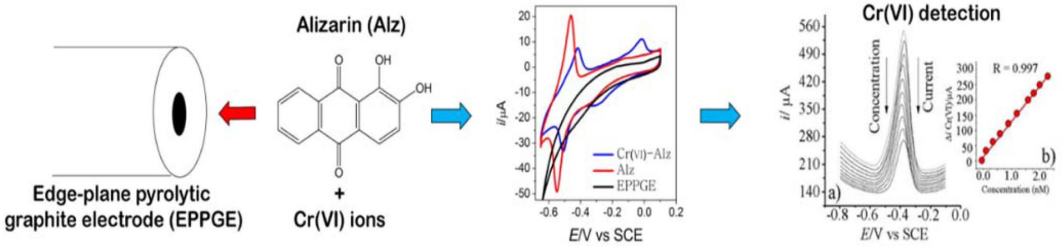

Fig. 6. Schematic illustration of the electrochemical role of alizarin compound.

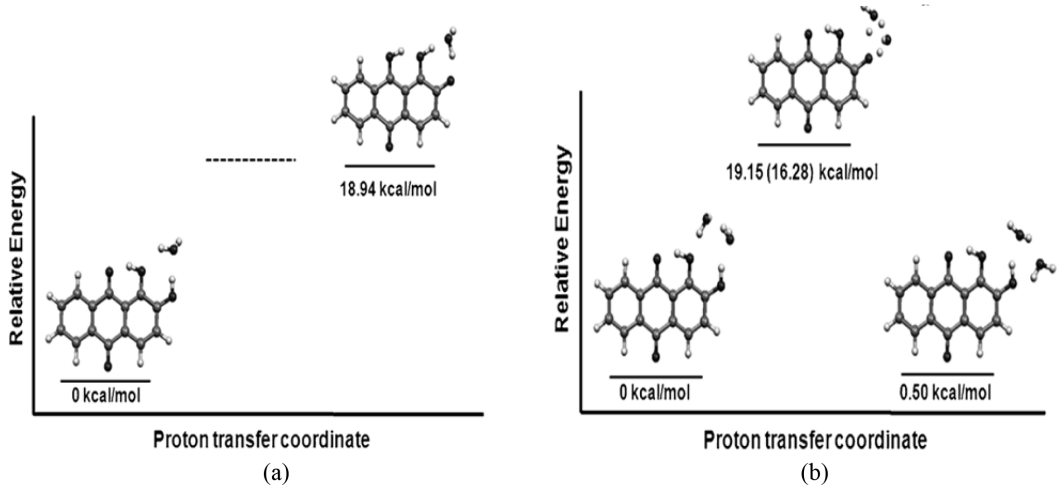

Fig. 7. Energy diagrams of the proton transfer reaction occurring in (a) $Az(H_2O)_1$ and (b) $Az(H_2O)_2$.[28]

graphite electrode (EPPGE) in terms of their electrochemical behaviors. The study was carried out at (5.10-6.52) range of pH to determine the highest voltametric response for the complex which was obtained at pH=6.52. Both the ligand and its metal-complex exhibited good electrochemical stability and high adsorption that is affected strongly by the pH of the electrolyte. The modification of the ligand with EPPGE enables the qualitative determination of chromium (VI) ions in Britton–Robinson buffer (aqueous medium) with 0.107 nmol L^{-1} detection limit. They obtained a linear response in the range of concentration (0.10 to 2.30 nmolL^{-1}). It can be concluded from this study that this system can be used as an ultra-trace levels electrochemical sensor of chromium (VI) ions.[27]

2.5. Hydrated alizarin complexes

Huh et al. (2012) studied the proton transfer and the structures of hydrogen bonding for the hydrated alizarin (Az) – complexes which was prepared in supersonic jet through utilizing fluorescence detected infrared spectroscopy (FDIR), hole burning (HB), dispersed laser induced fluorescence (LIF), and fluorescence excitation (FE). According to FDIR spectroscopic data, two different vibrational bands are acquired that are belonged to the two hydroxyl groups where the first one formed a strong hydrogen bonding as an intermolecular interaction, whereas the second group formed a weak hydrogen bonding interaction. They identify three conformations of $Az(H_2O)_1$ hydration complex with a ratio of 1:1. The conformation with the highest stability was forming hydrogen bonding with water molecule which behaves as proton donor for the first hydroxyl and proton acceptor for the second hydroxyl group. According to the quantum calculations, they suggested that the proton transfer occurs through electronic ground state

tunnelling for the excitation of the second hydroxyl group vibration of $Az(H_2O)_2$.[28]

3. Metal Complexes of Alizarin Derivatives

3.1. Gold (Ⅲ) complexes of alizarin and 3,4-dihydroxybenzaldehyde

Smith et al. (2016) prepared mixed ligand complexes of alizarin [Au(AZ)L] (where L=2-(p-tolyl)pyridyl (tolpy), 2-benzylpyridyl (bp), and 2-anilinopyridyl (anp)) from reacting of the complexes of cycloaurated gold(III) dichloride [$AuCl_2$(L)] with the alizarin [H_2AZ]. Moreover, they prepared [Au(dhb)(tolpy)] complexes from reacting of 3,4-dihydroxybenzaldehyde (H2dhb) and [$AuCl_2$(tolpy)]. These preparations of complexes introduce a new class of functionalities with ligands that linked through catecholate groups. Even though the solubility of these complexes in most solvents is very poor, they succeeded in characterizing the complexes using NMR, IR, MS, and ESI spectroscopic techniques. Two isomers are existed for the [Au(dhb)(tolpy)] complexes with respect to the aldehyde group position as concluded from the ^{1}H- and ^{13}C-NMR spectroscopic data.[29]

3.2. Inclusion complex of β-cyclodextrin and alizarin red S

Chin et al. (2015) studied the inclusion process of the Alizarin Red S (ARS) molecule in the b-cyclodextrin b-CD molecular cavity using cyclic voltammetry (CV), nuclear magnetic resonance (NMR), Fourier transform

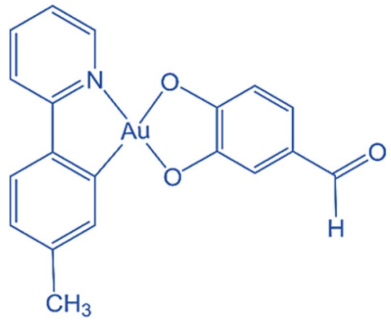

Fig. 8. Structure of gold (III) complexes of alizarin and 3,4-diydroxybenzaldehyde.[29]

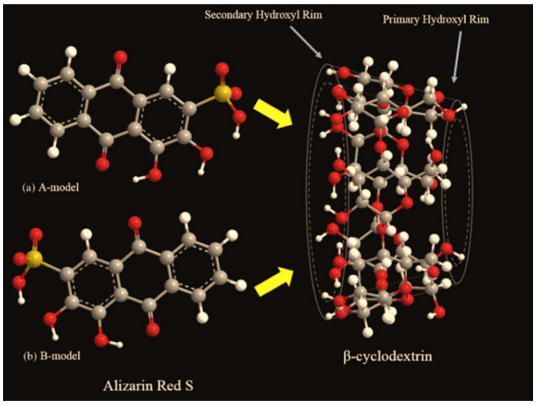

Fig. 9. Molecular orientation of b-cyclodextrin and Alizarin Red S.[30]

infrared (FTIR), UV–visible, and molecular modeling methods. Partly included ARS in the b-CD cavity was concluded according to the FTIR and NMR spectroscopic data forming a complex with 1:1 stoichiometry. They studied the most thermodynamically favorable orientation with the help of molecular modeling methods which implies that one of the force drive the formation of inclusion complex is the dipole-dipole interaction. According to the cyclic voltammetry, when the molecule of alizarin red s enters the cavity of b-CD, the current peak start decreasing. The study indicates that combining computational and experimental investigations provides enough details of the inclusion process of the formed complex.[30]

4. Pharmaceutical and Medicinal Applications

4.1. Alizarin for insulin fibrillation

Wang et al. (2021) studied using a model protein, in this case insulin, to investigate the antiamyloid effects of 1,2-dihydroxyanthraquinone (alizarin) and 1,2,4-trihydroxyanthraquinone (purpurin) which reported with highly bioactive compounds in terms of their antioxidation, antitumor, and antibacterial activity. It is rarely reported in the literature that these compounds can possess inhibiting effect against the aggregation of amyloid. According to this study, these two compounds exhibited high inhibition activity against

the insulin fibrils formation which depends on the doses of the compounds as well as reducing the induced cytotoxicity of insulin. Moreover, purpurin compound exhibited higher inhibition of amyloid fibrils of insulin in comparison with alizarin. Computational simulations showed the interaction between the two compounds with insulin chain B residues that are highly hydrophobic as well as interfering with the residues of phenylalanine binding as illustrated in *Fig.* 10. In conclusion, these two compounds possess play significant role in the prevention of the diseases that relate to protein misfolding as well as the high potential of utilizing as anti – amyloidosis drugs.[31]

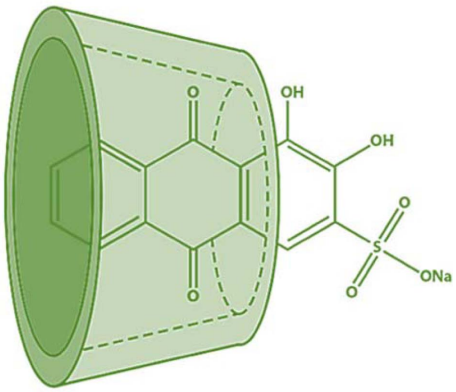

Fig. 10. Proposed structure of the inclusion complex.[30]

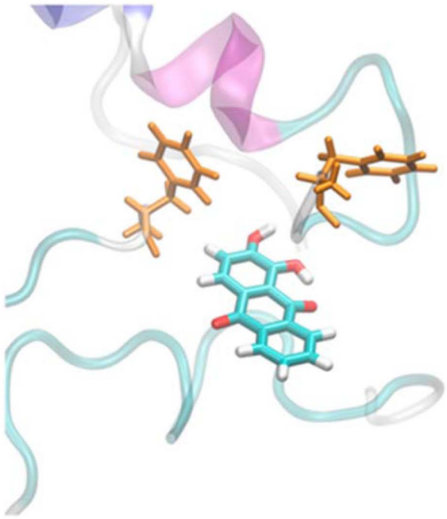

Fig. 11. Molecular model of insulin–alizarin system.[31]

5. Industrial Applications

5.1. Radical scavenging activity of alizarin

Jeremić et al. (2014) investigated the action of alizarin as radical scavenging from the thermodynamic and conformational behavior perspective by employing quantum computation that was carried out in water solution and gas phase. They examined radical cations and anions that resulted from alizarin by calculating the values of electron transfer enthalpy, proton affinity, proton dissociation enthalpy, ionization potential, and bond dissociation enthalpy. The calculations showed the preferred position for homolytic and heterolytic cleavage is the second hydroxyl group of alizarin according to the spin density (*Fig.* 12) and negative charge that delocalized in the second ring in case of radicals or anions form. It can be concluded from this study that even though the significantly low values of ionization potential, SET – PT can not be the favorable mechanism for alizarin in gas and water solution. SPLET, however, can represent the favorable mechanism in aqueous solution, whereas the reaction pathway in gas phase of alizarin can be attributed predominately as HAT.[32]

5.2. Hybrid pigments made from alizarin dye

Marzec et al. (2019) fabricated a novel hybrid

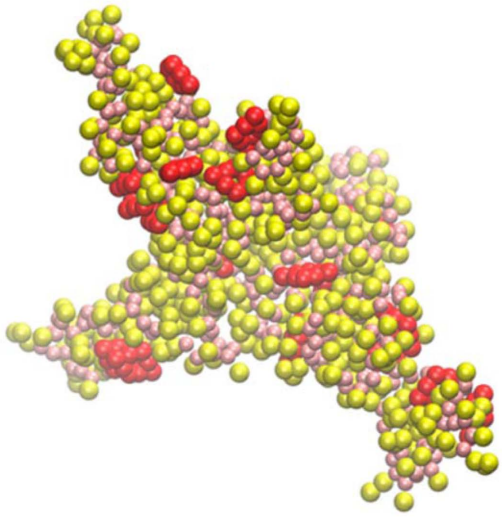

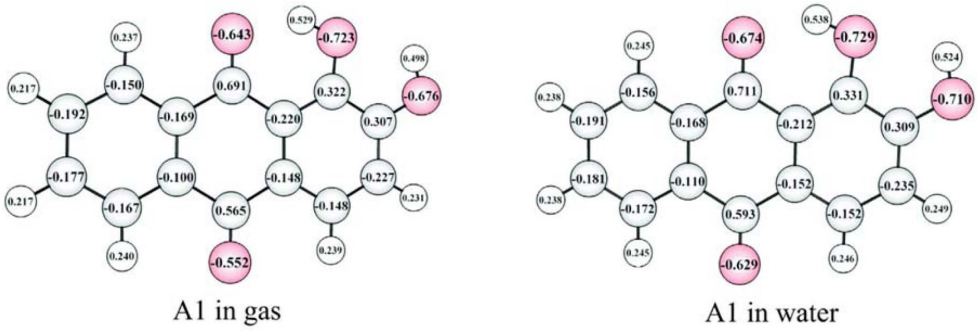

Fig. 12. Charge distribution of alizarin in the gaseous phase and aqueous solution.[32]

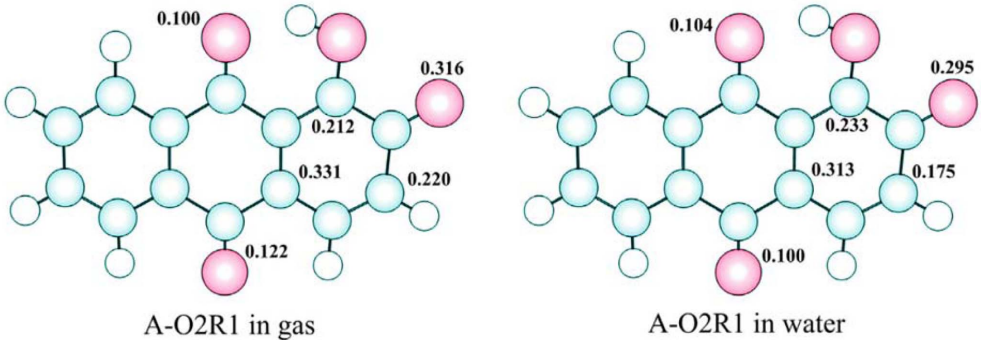

Fig. 13. Spin density distribution of alizarin in gaseous phase and aqueous solution.[32]

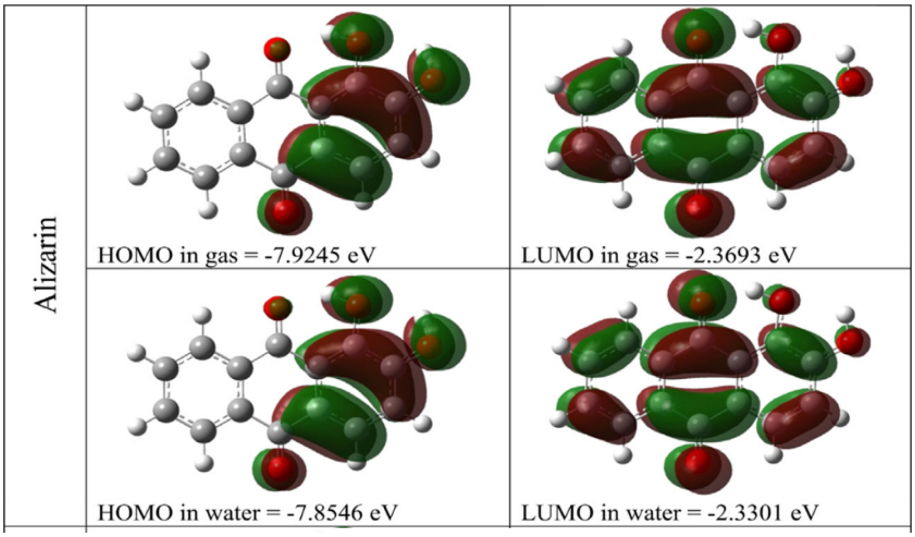

Fig. 14. Corresponding energies of alizarin in the gaseous phase and aqueous solution.[32]

pigment that derived from alizarin (1,2-dihydroxyanthraquinone) hosted on a magnesium – aluminum hydroxycarbonate mixed. Different techniques were used to investigate the organic (alizarin) – inorganic (metal oxides) interactions, including thermogravimetric analysis, X-ray diffraction, ^{27}Al – nuclear magnetic resonance, and TOF-SIMS ion mass spectroscopy. According to the TOF-Mass data, the success of

modifying the metal oxide was proved as it showed $C_{14}H_6O_5Al^-$ and $C_{14}H_7O_4Mg^+$ ions pecks which implied that the organic chromophore interacted with the oxide host. ^{27}Al–NMR spectra suggested that alizarin molecules interact with aluminum ions in the modified matrix as relative chemical shifts are detected. They observed color changing after the reaction with Al^{3+} and Mg^{2+} ions with significant improving in the color stability and dissolution resistance of alizarin at higher temperatures when compared to the pure dye. These physicochemical changes caused by the strong interaction between the dye and the metal oxide which transform effectively the dye into the insoluble form. When compared to the commercial form of the alizarin (Crimson), the modified pigments showed higher color stability with greater thermal resistance as illustrated in *Fig.* 14.[33]

5.3. The application of alizarin dye as aluminum ion detector

Chang (2010) developed a printed carbon electrode that is modified with alizarin red S dye as an organic chelating ligand in order to electrochemically detect aluminum ion in aqueous solution. Poly vinyl alcohol was used to immobilize the alizarin red S on the developed electrode for fabricating the sensor. Amperometric analytical technique was used to indirectly determine the immobilized aluminum concentration on the electrode that is not complexed after the complexation process with aluminum. The developed sensor has a detection limit of 25 μM and sensitivity of 3.8 nA $\mu M^{-1}cm^{-2}$.[34]

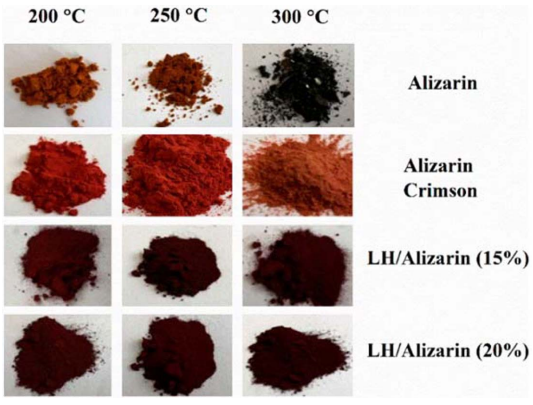

Fig. 15. Changing in color for hybrid pigments, the pure alizarin, and alizarin crimson at range of temperature from 200 to 300 °C.[3]

5.4. Alizarin removal from wastewater

Mukherjee et al. (2019) investigated of the usage of electrocoagulation (EC) process to remove (ARS) alizarin red S dye out of aqueous solution with applying Taguchi method for studying the parameters effects on removing ARS. They conducted the process in a electrochemically batched cell and the aluminum electrode is immerse in the dye solution by nonpolar connection. Many parameters were studied, including NaCl amount in terms of the distance between the inter-electrode and electrolyte, initial concentration of the dye, and the current intensity. They chose three levels for every parameter process for optimizing purpose and carried out the set of experiments at an ambient temperature and pH=7, as well as fixing the time at 20 min in order to determine the efficiency of removal. They found that the optimum conditions are; 3rd level for the initial concentration of NaCl (7 ppm), 1st level for dye initial concentration (10 ppm), 1st level for the distance between the interelectrode (0.6 cm), and 3rd level for the intensity of the current (4 A). The effeciciny of removal was determined at the optimum conditions to be 89.27%. At these optimized values, the removal of ARS was obtained at the maximum level. The researchers used ANNOVA package to prioritize the effect of parameters on ARS removal. [35]

5.5. Alizarin complex as A fluoride chemosensor

Jia et al. (2013) reported the ultrathin films of colorimetric molecule/double hydroxide layer which was fabricated using (LDH) LBL deposition process and they demonstrated the usage of these materials as fluoride colorimetric chemosensor. The studies UTF showed a stacking order as uniform and continuous in the substrate normal direction according to the surface morphology and structural analysis. Alizarin complex molecules are separated from each other using LDH nanoparticles. Regular and stepwise growth was

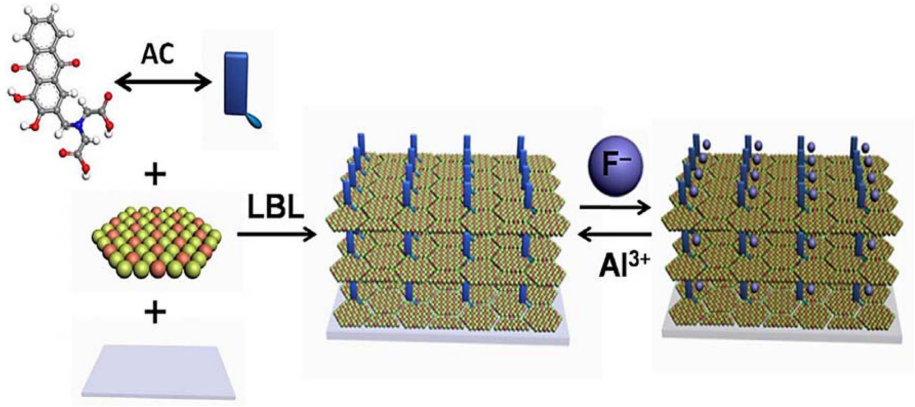

Fig. 16. The cycle of measurement–regeneration of alizarin complex/LDH.[36]

displayed by alizarin complex – LDH system as the UV-Vis spectroscopic data proved the increases in the deposition cycles. XRD and SEM data showed that periodical layered structures with bilayer thickness of 6.00 – 6.25 nm which are perpendicular to the substrates. Distinctive behavior was displayed by the alizarin complex with the LDH as a fluoride colorimetric chemosensor. Furthermore, this chemosenser has high selectivity, stability, good reversibility and regeneration, as well as a low detection limit of 12.9 μM. The measuring – regenerating cycle mechanism that they proposed for the chemosensor includes fluoride entering and departing from the alizarin complex – LDH system with high changing reversibility in the surface morphology and chemical composition of the UTF. *Fig.* 15 illustrates the mechanism of alizarin complex – LDH work as a chemosensor.[36]

6. Conclusions

This literature review displayed the importance of synthesizing new metal-complexes of alizarin as well as new derivatives which can be very advantageous in many applications such as bioactive materials with high anti-cancer, anti-microbial, and anti-viral properties. Moreover, many other applications can be noticed in the latest studies of alizarin-complexes which showcase the importance of these materials. These studies encourage the researchers to pay more attention for synthesizing and studying the properties of these materials.

References

1. T. Jeliński and P. Cysewski, *J. Mol. Model.*, **22**(6), 1-10 (2016).
2. L. G. Angelini, L. Pistelli, P. Belloni, A. Bertoli, and S. Panconesi, *Ind. Crops. Prod.*, **6**(3-4), 303-311 (1997).
3. S. Murcia-Mascarós, C. Domingo, S. Sanchez-Cortes, M. Canamares, and J. Garcia-Ramos, *J. Raman Spectrosc.*, **36**(5), 420-426 (2005).
4. R. Sánchez-de-Armas, J. Oviedo Lopez, M. A. San-Miguel, J. F. Sanz, P. Ordejón, and M. Pruneda, *J. Chem. Theory Comput.*, **6**(9), 2856-2865 (2010).
5. V. Y. Fain, B. Zaitsev, and M. Ryabov, *Russ. J. Coord. Chem.*, **30**(5), 365-370 (2004).
6. S. Das, A. Bhattacharya, P. Mandal, M. Rath, and T. Mukherjee, *Radiat. Phys. Chem.*, **65**(1), 93-100 (2002).
7. H. M. Berman and P. R. Young, *Annu. Rev. Biophys.*, **10**(1), 87-114 (1981).
8. M. Canamares, J. Garcia-Ramos, C. Domingo, and S. Sanchez-Cortes, *J. Raman Spectrosc.*, **35**(11), 921-927 (2004).
9. W. A. Remers, 'Chemistry of Antitumor Antibiotics', Wiley, New Jersey, 1979.
10. R. H. Thomson, 'Naturally Occurring Quinones Volume III', 3rd Ed., Chapman & Hall, London, 1987.
11. J. R. Choi, S. C. Jeoung, and D. W. Cho, *Chem. Phys. Lett.*, **385**(5-6), 384-388 (2004).
12. T. D. Giacco, L. Latterini, and F. Elisei, *Photochem. Photobiol. Sci.*, **2**(6), 681-687 (2003).
13. C. Miliani, A. Romani, and G. Favaro, *J. Phys. Org.*

Chem., **13**(3), 141-150 (2000).
14. L. Quinti, N. S. Allen, M. Edge, B. P. Murphy, and A. Perotti, *J. Photochem. Photobiol. A*, **155**(1-3), 79-91 (2003).
15. T. H. Al-Noor, *Ibn al-Haitham J. Pure Appl. Sci.*, **19**(3), 85-98 (2006).
16. S. Sharma, P. Mishra, and O. Rai, *Orient. J. Chem.*, **30**(4), 2011 (2014).
17. H. A. Hasan and E. I. Yousif, *Ibn al-Haitham J. Pure Appl. Sci.*, **29**(3), 146-166 (2017).
18. A. J. Al-Sarray, I. M. H. Al-Mousawi and T. H. Al-Noor, *Chem. Methodol.*, **6**(4), 331-338 (2022).
19. M. El-Nahass, H. Zeyada, N. El-Ghamaz, and A. Awed, *Optik*, **170**, 304-313 (2018).
20. H. Fujikawa, S. Yamaguchi, and K. Matsui, *Trans. Mater. Res. Soc. Jpn.*, **43**(3), 197-200 (2018).
21. E. I. Yousif and H. A. Hasan, *Ibn al-Haitham J. Pure Appl. Sci.*, **30**(1), 73-87 (2017).
22. V. Gomathi and R. Selvameena, *Inorganica Chim. Acta*, **480**, 42-46 (2018).
23. A. Królicka, J. Zarębski, and A. Bobrowski, *Chemosensors*, **10**(1), 36 (2022).
24. G. Valarmathy, R. Subbalakshmi, R. Sumathi, and R. Renganathan, *J. Mol. Struct.*, **1199**, 127029 (2020).
25. S. Martínez-Vargas, P. Gómez-Tagle, and A. K. Yatsimirsky, *Inorganica Chim. Acta*, **373**(1), 226-232 (2011).
26. F. Jumean, M. El-Dakiky, A. Manassra, M. A. Kareem, M. A. Alhaj, and M. Khamis, *Am. J. Analyt. Chem.*, **5**(1), 1-7 (2014).
27. N. J. S. Furtado, E. A. de Oliveira Farias, C. Eiras, J. L. Magalhães, and J. B. Silva, *Surf. Interfaces*, **14**, 238-244 (2019).
28. H. Huh, S. H. Cho, J. Heo, N. J. Kim, and S. K. Kim, *Phys. Chem. Chem. Phys.*, **14**(25), 8919-8924 (2012).
29. T. S. Smith, J. R. Lane, M. R. Mucalo, and W. Henderson, *Transit. Met. Chem.*, **41**(5), 581-589 (2016).
30. Y. P. Chin, S. F. A. Raof, S. Sinniah, V. S. Lee, S. Mohamad, and N. S. A. Manan, *J. Mol. Struct.*, **1083**, 236-244 (2015).
31. W. Wang, J. Zhang, W. Qi, R. Su, Z. He, and X. Peng, *ACS Chem. Neurosci.*, **12**(12), 2182-2193 (2021).
32. S. Jeremić, N. Filipović, A. Peulić, and Z. Marković, *Comput. Theor. Chem.*, **1047**, 15-21 (2014).
33. A. Marzec, B. Szadkowski, J. Rogowski, W. Maniukiewicz, M. I. Szynkowska, and M. Zaborski, *Materials*, **12**(3), 360 (2019).
34. S.-C. Chang, *J. Sens. Sci. Technol.*, **19**(6), 421-427 (2010).
35. T. Mukherjee, P. Das, S. K. Ghosh, and M. Rahaman, 'Waste Water Recycling and Management', Springer, Berlin, 2019.
36. Y. Jia, Z. Li, and W. Shi, *Sens. Actuators B Chem.*, **188**, 576-583 (2013).

Authors' Positions

Laith Jummah Al-Gburi : Graduate Student
Taghreed Hashim Al-Noor : Professor